Publication V

N. Chekurov, K. Grigoras, L. Sainiemi, A. Peltonen, I. Tittonen, and S. Franssila. 2010. Dry fabrication of microdevices by the combination of focused ion beam and cryogenic deep reactive ion etching. Journal of Micromechanics and Microengineering, volume 20, number 8, 085009, 6 pages.

© 2010 Institute of Physics Publishing (IOPP)

Reprinted by permission of Institute of Physics Publishing.

J. Micromech. Microeng. **20** (2010) 085009 (6pp) doi:10.1088/0960-1317/20/8/085009

Dry fabrication of microdevices by the combination of focused ion beam and cryogenic deep reactive ion etching

N Chekurov[1,4], K Grigoras[2], L Sainiemi[2], A Peltonen[3], I Tittonen[1] and S Franssila[2]

[1] Department of Micro and Nanosciences, School of Science and Technology, Aalto University, PO Box 13500, FI-00076 Aalto, Finland
[2] Department of Materials Science and Engineering, School of Science and Technology, Aalto University, PO Box 1620, FI-00076 Aalto, Finland
[3] Aalto Nanofab, School of Science and Technology, Aalto University, PO Box 13500, FI-00076 Aalto, Finland

E-mail: nikolai.chekurov@tkk.fi

Received 26 March 2010, in final form 31 May 2010
Published 2 July 2010
Online at stacks.iop.org/JMM/20/085009

Abstract
In this paper, we demonstrate silicon microdevice fabrication by a combination of focused ion beam (FIB) and cryogenic deep reactive ion etching (DRIE). Applying FIB treatment only to a thin surface layer enables very high writing speed compared with FIB milling. The use of DRIE then defines the micro- and nanodevices utilizing the FIB-modified silicon as a mask. We demonstrate the ability to create patterns on highly 3D structures, which is extremely challenging by other nanofabrication methods. The alignment of optically made and FIB-defined patterns is also demonstrated. We also show that complete microelectromechanical systems (MEMS) can be fabricated by this method by presenting a double-ended tuning fork resonator as an example. Extremely short process time is achieved as the full fabrication cycle from mask design to electrical measurements can be completed during one working day.

(Some figures in this article are in colour only in the electronic version)

1. Introduction

Testing of physical concepts that are based on structures that are well below 1 μm in size is a challenging task and often requires advanced high-resolution lithography and fabrication methods. Mass production techniques such as stepper lithography or nanoimprinting require slow and expensive mask or master fabrication. The conventional prototyping approaches include serial writing techniques such as electron beam lithography (EBL) and focused ion beam (FIB) milling as well as various self-assembly-based solutions [1]. The serial writing methods can produce arbitrary shapes, but they suffer from slow writing speed and a small writable area. On the other hand, the self-assembly methods are usually restricted only to the limited complexity of features and are prone to defects [1].

FIB milling, etching and deposition are established micro- and nanofabrication techniques [2–4]. As milling relies solely on ion sputtering of the material, deposition and chemically assisted etching are achieved by introducing gaseous chemicals to the processing chamber. Those chemicals react with the ion beam and decompose from their passive state either into deposited material or to etching agents. In the case of silicon, the use of Cl_2, Br_2 or I_2 can amplify the sputtering yield and speed up the processing by a maximum factor of 8 [5], leading, however, to somewhat lower resolution compared to pure milling.

FIB processing speed can be greatly improved by a doping approach (instead of direct milling) and using etching techniques that exhibit selectivity between doped and undoped

[4] Author to whom any correspondence should be addressed.

 © 2010 IOP Publishing Ltd Printed in the UK & the USA

regions of a silicon substrate [6–9]. In this way, only a thin top layer of the substrate needs to be treated by FIB, and most of the material is removed in a subsequent etching step, enhancing the speed by orders of magnitude compared to conventional milling. The speed enhancement is most significant in the case of dark field structuring, where a lot of material has to be removed and only small areas have to be protected. We have shown earlier [9] that gallium-doped silicon can serve as an etch mask in plasma etching of high aspect ratio nanopillars.

This work is divided into two parts. First, we demonstrate the suitability of the masking method for the modification of thermal microbridge actuators, which were fabricated by standard optical lithography. The actuators are suspended microbridges hundreds of micrometers long, but only a few micrometers wide and 4 μm thick [10]. Applying a thin photoresist layer on top of a wafer with suspended structures is impossible, and therefore direct masking or etching methods are the only possible means to modify the devices.

In the second part, we demonstrate a double-ended tuning fork resonator created in an all-dry process by the FIB/DRIE (deep reactive ion etching) method. When DRIE reaches the buried oxide in a silicon-on-insulator (SOI) wafer, the horizontal etching of silicon takes place due to ion deflection. This notching effect (a.k.a. footing effect) was employed to release the moving parts of the device [11, 12].

For the notching effect to appear, rather long etching times have to be used. The excellent masking properties of the Ga^+-doped layer enable etching times of at least 40 min without any mask failure. This is enough to undercut several microns under typical conditions [9].

Eliminating all the wet steps such as photoresist spinning and baking remarkably speeds up the fabrication cycle, even compared with processes based on EBL.

2. Experimental setup

In our experiments, a Helios Nanolab 600 dual beam system (FEI Company) was used. A liquid metal source was utilized to generate a Ga^+ ion beam with currents between 1.5 pA and 21 nA. The minimum dwell time was 50 ns, and maximum 4.6 ms. The beam voltage was kept at 30 keV. The maximum field of view, which determines the largest writable structure, was about 700 × 700 μm^2. The whole area can be modified into an etch-resistant state in less than 17 min using maximum ion current. Depending on the pattern density even a few seconds can suffice.

The DRIE experiments were carried out in a Plasmalab System 100 reactor (Oxford Instruments). The system has two power sources: high-density SF_6/O_2 plasma is generated with an inductively coupled plasma (ICP) source while ion energies are controlled separately with a capacitively coupled plasma (CCP) source, both operating at 13.56 MHz. Mechanical clamping of the wafer and helium backside cooling ensure the effective heat exchange between the liquid nitrogen-cooled electrode and the wafer. The standard etching conditions were: temperature $T = -120$ °C, pressure $p = 9$ mTorr, ICP power $P_{ICP} = 800$ W, CCP (forward) power $P_{CCP} = 3$ W, gas mixture SF_6/O_2 40/6.5 sccm, etch rate about 2 μm min^{-1} [9].

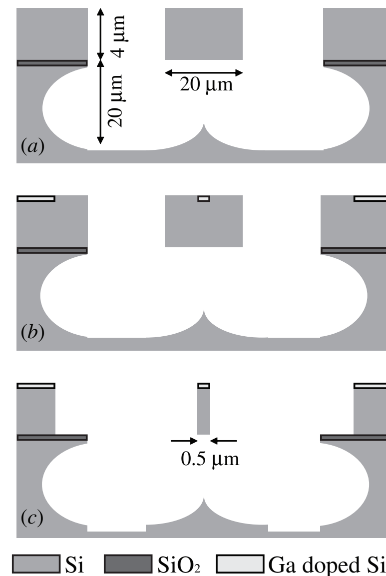

Figure 1. Thermal actuator modification. (*a*) The original actuator, (*b*) a gallium doping layer is aligned and implanted with FIB, and (*c*) the final structure after DRIE. Images show the cross-sectional profile of the beams and the underlying structure.

3. Thermal actuator modification

The thermal actuators were originally fabricated using photolithography and DRIE with an isotropic plasma etch step for release [10]. Figure 1 shows the modification process. We start with a released bridge structure (figure 1(*a*)) and dope by FIB the shape of a final device (figure 1(*b*)), and finally etch undoped silicon away with anisotropic DRIE (figure 1(*c*)). Figure 2 shows an electron micrograph of an actuator prior to modification (figure 2(*a*)), after the doping of the masking layer (figure 2(*b*)) and after DRIE (figure 2(*c*)). A close-up of the final modified structure shows the wall and masking quality (figure 2(*d*)). The ion dose required to protect the structures is in the order of 2 × 10^{16} ions cm^{-2} [9], so using the ion current of 9.7 pA, it takes about 400 s to create a masking layer for one 100 μm × 0.5 μm bridge. By adjusting the current, this time may be shortened or prolonged depending on the required resolution. By choosing the exposure time properly, we can get an advantage of near-perfect alignment, as several quick (0.05 s/frame) ion images of the region of interest can be taken. The dose is not high enough to create an etch stop layer. Using the ion image as a background map, it is straightforward to align structures with submicron accuracy (figure 3). A pillar on top of the bridge is a result of re-focusing the ion column; the process of beam adjustment is quite time consuming and the sacrificial focusing site was implanted enough to act as a masking layer.

In this experiment, two separate steps were applied to mask the structures. First, connections to the bonding pads were irradiated. Because of their big size (2 × 120 μm × 50 μm) and low accuracy requirements, the highest current of 19 nA was used. The areas were irradiated for 38 s which yields the implantation dose of 2.7 × 10^{16} ions cm^{-2}. In the second step, high-resolution bridges were patterned using the

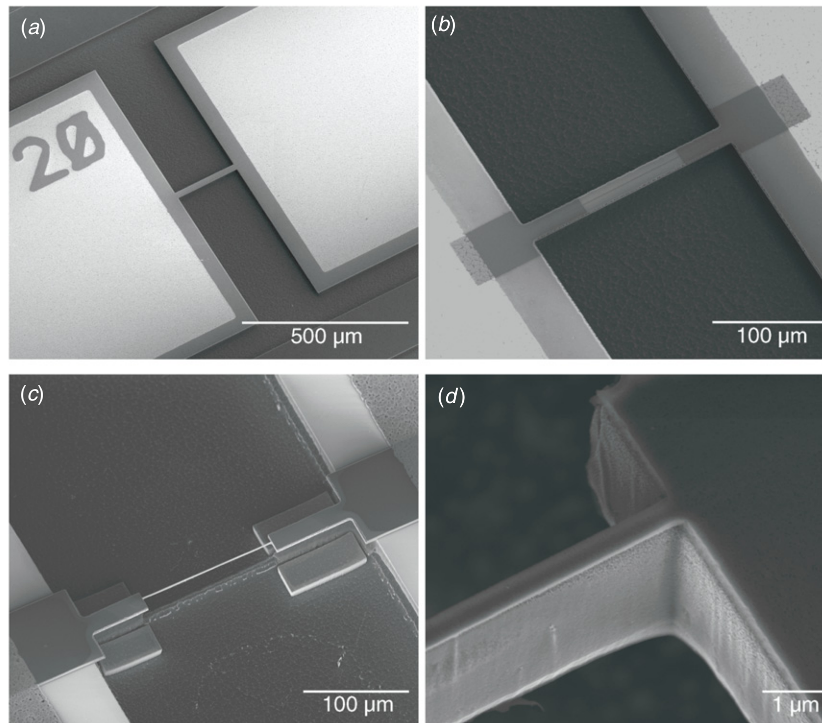

Figure 2. Electron micrographs of a modified microactuator. (*a*) A thermal microactuator prior to modification (200 μm × 25 μm × 4 μm), (*b*) actuator masked by Ga^+ doping, (*c*) modified actuator with the middle section of the bridge narrowed using the FIB/DRIE method; the dimensions of the middle sections are (100 μm × 0.36 μm × 4 μm), and (*d*) a close-up on the modified actuator showing the masking and wall quality.

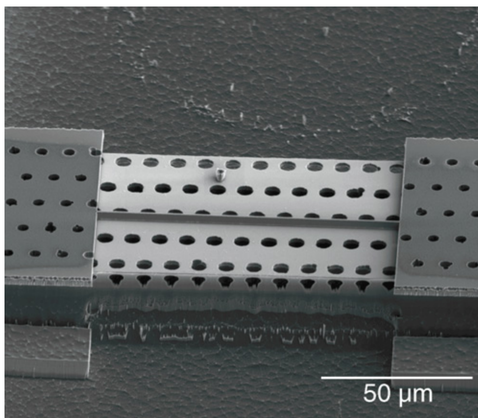

Figure 3. A 0.5 μm × 100 μm size bridge precisely positioned between the holes on a photolithographically fabricated released perforated structure.

beam current of 23 pA and the dose of 5 × 10^{16} ions cm^{-2}. During this step, the patterns were aligned to the pre-made structures by the method described above.

For comparison, similar microactuators were modified by a pure physical milling and the results are shown in figure 4. Milling two 100 μm long and 7.5 μm wide parts of the bridge took 25 min at maximum current (19 nA), and final polishing with 7.9 nA an extra 10 min. The polishing improves the corner quality between the top surface and the sidewall of the bridge, but even with polishing the final result is inferior to DRIE etched (figures 4(*b*) and 2(*d*)).

One way to characterize the thermal microbridge actuators is to measure their IV curves, which are affected by the geometry and material of the bridges [10]. Figure 5 shows the measurement results for an unmodified structure as well as FIB/DRIE-modified and FIB milled ones.

Silicon microbridges typically exhibit power–resistance (RP) characteristics with a well-defined peak in resistance R_{peak} when enough power is applied to reach the temperature of intrinsic conductivity of silicon (figure 5(*a*)). R_{peak} temperature is the same for all bridges that have the same doping level [13]. The required power depends on the width of the bridge as shown in figure 5(*b*), and both the results of unmodified and modified bridges are set in the same plot, forming a continuous line. 5 μm wide bridges were fabricated in all three ways—with photolithography, by modifying wider bridges with FIB/DRIE process and by physical FIB milling. For all those bridges, the power requirement to reach R_{peak} is almost identical.

As a conclusion, we can say that modifying the structures by either way did not alter the functionality of the structures as gallium doping does not significantly change the conductivity of devices because the modified layer is only about 30 nm thick (<1% of bridge thickness). Even milling the bridge directly, inducing gallium doping on three sides of the bridge does not drastically change the conductivity of the final structures.

4. All-dry MEMS fabrication

As a second demonstration, we fabricate a fully operational microdevice using the FIB/DRIE fabricating technique. We

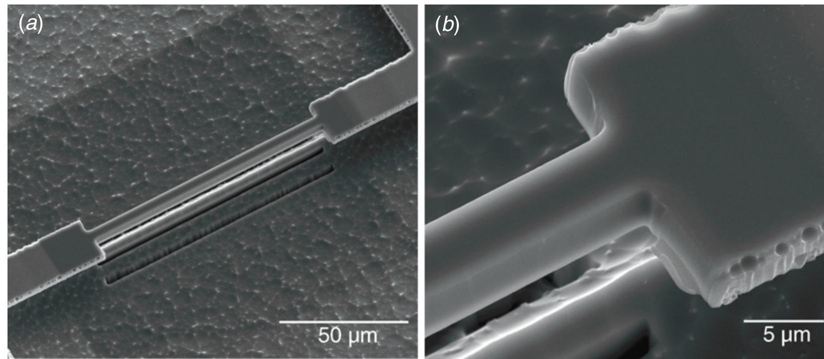

Figure 4. Bridge modification by conventional FIB-milling. (*a*) Overview of the modified bridge, and (*b*) close-up showing the side wall quality.

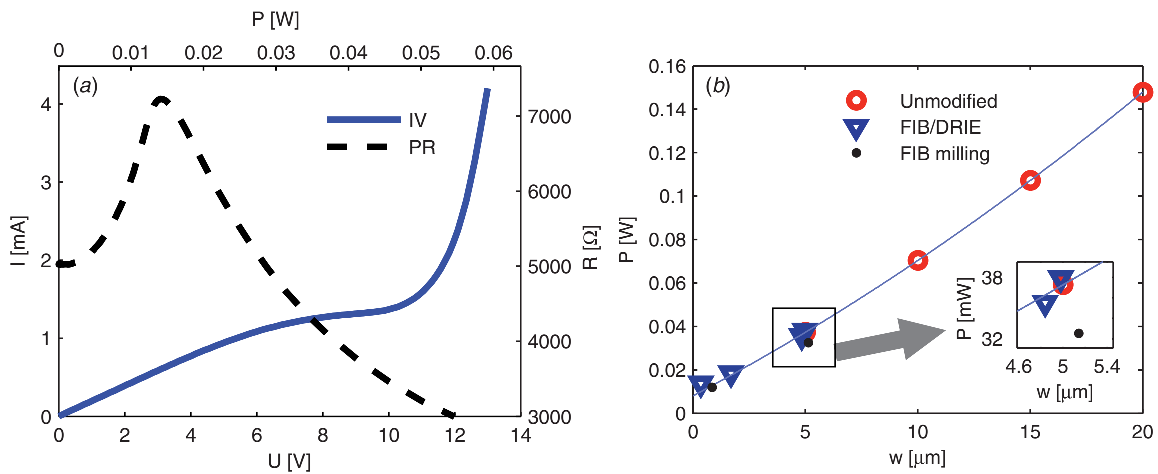

Figure 5. Measured electrical properties of microactuators. (*a*) Measured IV and RP–curves of a modified 360 nm × 100 μm × 4 μm bridge, and (*b*) power required for reaching the maximum resistance as a function of bridge width.

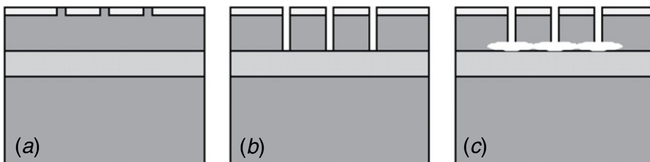

Figure 6. Fabrication of a micro mechanical resonator utilizing the notching effect on an SOI wafer: (*a*) FIB masking, (*b*) etch end point, and (*c*) release of the structures utilizing the notching effect during overetching.

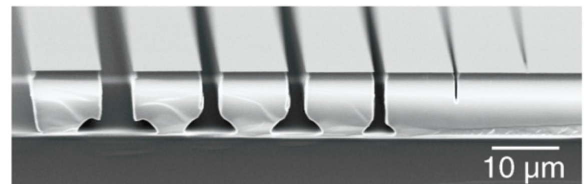

Figure 7. Notching release test. Dimensions of the gaps on a mask from left to right: 5 μm, 3 μm, 2 μm, 1 μm, 0.5 μm. Gap width in silicon: 5 μm, 3 μm, 3 μm, 2 μm, 0.67 μm. Maximum released width: 3.55 μm, 2.5 μm, 2.5 μm, 1.5 μm, 0 μm.

utilized an all-dry notching method in the fabrication of double-ended tuning fork resonators (figure 6). One of the key properties of the capacitively coupled MEMS is the width of the coupling gap, *d*. With local gallium-doped masking, the gap size can be as small as 50 nm but the final structure size is usually limited by the aspect ratio achievable in etching. With cryogenic DRIE, ratios of 20:1 are typical [14], which transfers to 500 nm gap for 10 μm SOI device layer thickness. In our case, the gap size was optimized to maximize the notching effect and ensure the proper release of the component (figure 7).

The resonator topology was chosen to be of double-ended tuning-fork (DETF) type with the length $L = 100$ μm, width $w = 2$ μm, distance between the branches $a = 1$ μm and a coupling gap width $d = 2$ μm (figure 8). The whole resonator, including the bonding pads, was written in less than 17 min using the maximum 19 nA ion current and etched in less than 10 min.

The eigenfrequency analysis of the structure was performed using the COMSOL finite element modeling software using Young's modulus $E = 131$ GPa ([1 0 0] direction) and density $r = 2330$ kg m^{-3} for silicon. The modeled frequencies for in-phase and anti-phase modes were $f_{\text{in-phase}} = 1.58$ MHz and $f_{\text{anti-phase}} = 1.66$ MHz, respectively. The simulated modes of vibration are shown in figure 9.

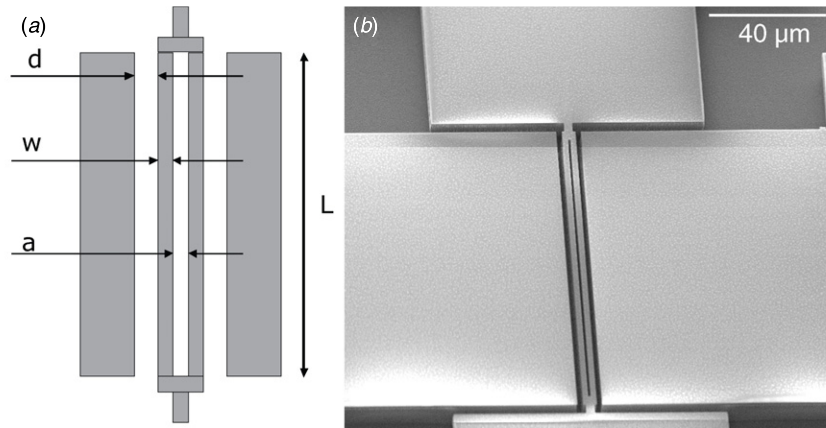

Figure 8. (*a*) A schematic view of the final resonator structure: $d = 2\ \mu$m, $w = 2\ \mu$m, $a = 1\ \mu$m, $L = 100\ \mu$m, $h = 10\ \mu$m, and (*b*) a micrograph of a fabricated resonator.

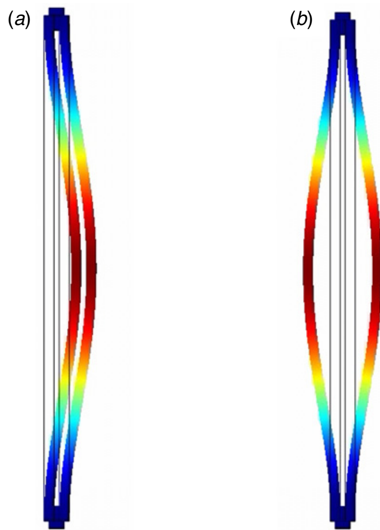

Figure 9. Simulated vibration modes of a DETF resonator. (*a*) In-phase mode $f_{\text{in-phase}} = 1.58$ MHz, and (*b*) anti-phase mode $f_{\text{anti-phase}} = 1.66$ MHz.

The frequency response of the fabricated resonator was measured, and both the modeled resonances were found to be present (figure 10) indicating that the release has been successful. The measured frequencies of the modes were $f_{\text{in-phasemeasured}} = 1.48$ MHz and $f_{\text{anti-phasemeasured}} = 1.62$ MHz which is within 10% of the simulated values.

5. Conclusion

One of the major limitations of FIB technology is its slow milling speed, as removing a few tens of thousands μm^3 of material takes hours, even in a gas-assisted mode. In this paper, we utilized such an approach where only a thin top layer of a structure needs to be treated by FIB, speeding up the processing by several orders of magnitude. The material removal is carried out in a subsequent DRIE step. The dose required to protect silicon during the etching step is equivalent to milling 3–7 nm of the material. Obviously, there is a need for a DRIE system to take benefit of this 2D FIB patterning. Fabrication of released, free-standing MEMS and NEMS structures is highly suitable for the FIB/DRIE method because it sidesteps all wet processes, eliminating stiction.

Mix-and-match of optical lithography and FIB/DRIE patterning on 3D released microstructures has been shown to work. This opens up possibilities of speeding up nanostructuring because coarse structures can be made using

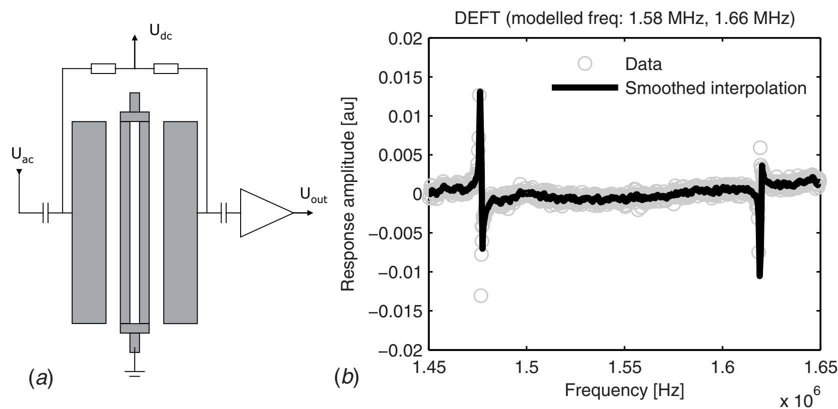

Figure 10. (*a*) Measurement scheme, and (*b*) frequency response of a DETF resonator.

optical lithography, and then fine-tuned by the FIB/DRIE method.

We have also shown that the described method can be used for fabricating electrostatically coupled MEMS in a simple, all-dry two-step process, during a working day from mask design to RF-measurements.

The future prospects include extending the technique to fabricating sub-100 nm structures such as low-voltage nanoresonators using thin SOI device layers.

Acknowledgments

This work was funded by Academy of Finland (project nos 123708, 134506). Dr Mika Koskenvuori is acknowledged for performing measurements on MEMS resonators. Dr Veli-Matti Airaksinen at Micronova clean room facility is acknowledged for fruitful collaboration.

References

[1] Lu W and Sastry A M 2007 Self-assembly for semiconductor industry *IEEE Trans. Semicond. Manuf.* **20** 421
[2] Reytjens S and Puers R 2001 A review of focused ion beam applications in microsystem technology *J. Micromech. Microeng.* **11** 287
[3] Tseng A 2004 Recent developments in micromilling using focused ion beam technology *J. Micromech. Microeng.* **14** R15
[4] Utke I, Hoffmann P and Melngailis J 2008 Gas-assisted focused electron beam and ion beam processing and fabrication *J. Vac. Sci. Technol.* **26** 1197
[5] Ray V 2004 Fluorocarbon precursor for high aspect ratio via milling in focused ion beam modification of integrated circuits *30th Int. Symp. for Testing and Failure Analysis* p 534
[6] Qian H X, Zhou W, Miao J, Lim L E N and Zeng X R 2008 Fabrication of Si microstructures using focused ion beam implantation and reactive ion etching *J. Micromech. Microeng.* **18** 035003
[7] Bischoff L, Schmidt B, Lange H and Donzev D 2009 Nano-structures for sensors on SOI by writing FIB implantation and subsequent anisotropic wet chemical etching *Nucl. Instrum. Methods Phys. Res.* B **267** 1372–5
[8] Sievilä P, Chekurov N and Tittonen I 2010 The fabrication of silicon nanostructures by focused-ion-beam implantation and TMAH wet etching *Nanotechnology* **21** 145301
[9] Chekurov N, Grigoras K, Peltonen A, Franssila S and Tittonen I 2009 The fabrication of silicon nanostructures by local gallium implantation and cryogenic deep reactive ion etching *Nanotechnology* **20** 065307
[10] Sainiemi L, Grigoras K, Kassamakov I, Hanhijarvi K, Aaltonen J, Fan J, Saarela V, Haeggstrom E and Franssila S 2009 Fabrication of thermal microbridge actuators and characterization of their electrical and mechanical responses *Sensors Actuators* A **149** 305–14
[11] Franssila S, Kiihamäki J and Karttunen J 2000 Etching through silicon wafer in inductively coupled plasma *Microsyst. Technol.* **6** 141
[12] Chekurov N, Koskenvuori M, Airaksinen V-M and Tittonen I 2007 Atomic layer deposition enhanced rapid dry fabrication of micromechanical devices with cryogenic deep reactive ion etching *J. Micromech. Microeng.* **17** 1731
[13] Shpak M, Sainiemi L, Ojanen M, Kärhä P, Heinonen M, Franssila S and Ikonen E 2010 Optical temperature measurements of silicon microbridge emitters *Appl. Opt.* **49** 1489–93
[14] Sainiemi L, Keskinen H, Aromaa M, Luosujärvi L, Grigoras K, Kotiaho T, Mäkelä J M and Franssila S 2007 Rapid fabrication of high aspect ratio silicon nanopillars for chemical analysis *Nanotechnology* **18** 505303